Hindawi Publishing Corporation
Journal of Nanomaterials
Volume 2013, Article ID 173232, 9 pages
http://dx.doi.org/10.1155/2013/173232

Research Article

Improved Methane Sensing Properties of Co-Doped SnO_2 Electrospun Nanofibers

Weigen Chen,[1] Qu Zhou,[1] Lingna Xu,[1] Fu Wan,[1] Shudi Peng,[2] and Wen Zeng[1,3]

[1] *State Key Laboratory of Power Transmission Equipment & System Security and New Technology, Chongqing University, Chongqing 400030, China*
[2] *Chongqing Electric Power Research Institute, Chongqing 401123, China*
[3] *College of Materials Science and Engineering, Chongqing University, Chongqing 400030, China*

Correspondence should be addressed to Weigen Chen; weigench@cqu.edu.cn and Qu Zhou; zhouqu@cqu.edu.cn

Received 11 July 2013; Revised 23 September 2013; Accepted 7 October 2013

Academic Editor: Gajanan S. Bhat

Co-doped SnO_2 nanofibers were successfully synthesized via electrospinning method, and Co-doped SnO_2 nanospheres were also prepared with traditional hydrothermal synthesis route for comparison. The synthesized SnO_2 nanostructures were characterized by X-ray powder diffraction, scanning electron microscopy, transmission electron microscopy, energy dispersive X-ray spectroscopy, and X-ray photoelectron spectra. Planar-type chemical gas sensors were fabricated and their sensing properties to methane were investigated in detail. Gas sensors based on these two samples demonstrate the highest CH_4 sensing response at an operating temperature of 300°C. Compared with traditional SnO_2 nanospheres, the nanofiber sensor shows obviously enhanced gas response, higher saturated detection concentration, and quicker response-recovery time to methane. Moreover, good stability, prominent reproducibility, and excellent selectivity are also observed based on the nanofibers. These results demonstrate the potential application of Co-doped SnO_2 nanofibers for fabricating high performance methane sensors.

1. Introduction

As an interesting chemically and thermally stable n-type semiconductor with wide band gap energy and large exciton binding energy, tin oxide (SnO_2) has attracted increasing attention and been extensively studied for catalysis [1], solar cells [2], optoelectronics [3], lithium-ion batteries [4], chemical sensors [5, 6], and so on [7–9]. Moreover, it has been proved to be a highly sensitive material for the detection of both reducing and oxidizing gases [10, 11]. Since the gas sensing properties of SnO_2-based sensors are closely related to the reactions between gas molecules and SnO_2 surfaces, interest in tailoring the microstructure and morphology of SnO_2 nanostructures has been greatly stimulated [12–14]. Over the past years, many scientific and technological efforts have been made to improve the sensitivity, response-recovery characteristic, selectivity, and stability of SnO_2-based sensors [15–17].

Recently, one-dimensional (1D) [18, 19] and quasi-one-dimensional [20] SnO_2 nanostructures with different morphologies including nanorods [21], nanotubes [22], nanowires [23], nanobelts [24], nanosheets [25], and nanofibers [26, 27] have been successfully fabricated and reported. Taking advantage of the small grain size, large surface-to-volume ratio, high density of surface sites, special hole, and pore structure, these novel low-dimensional SnO_2 nanostructures demonstrate excellent gas sensing performances than those of traditional SnO_2 nanoparticles or thin films. Currently, electrospinning [10, 11, 28, 29], sol-gel method [5], thermal evaporation technology [30], hydrothermal method [31], and chemical vapor deposition [32] are the main methods used to synthesize low-dimensional oxide nanostructures. Among all the fabrication techniques, electrospinning [17, 28] has been demonstrated as a relatively facile and versatile method for the large-scale synthesis of 1D

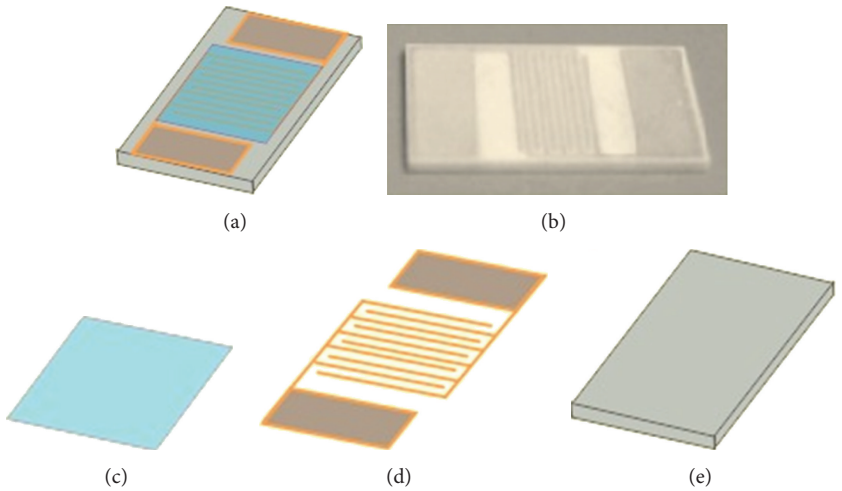

Figure 1: Structure chart of the planar sensor. (a) A top view of the substrate, (b) fabricated gas sensor, (c) sensing materials, (d) Ag-Pd interdigital electrodes, and (e) ceramic substrate.

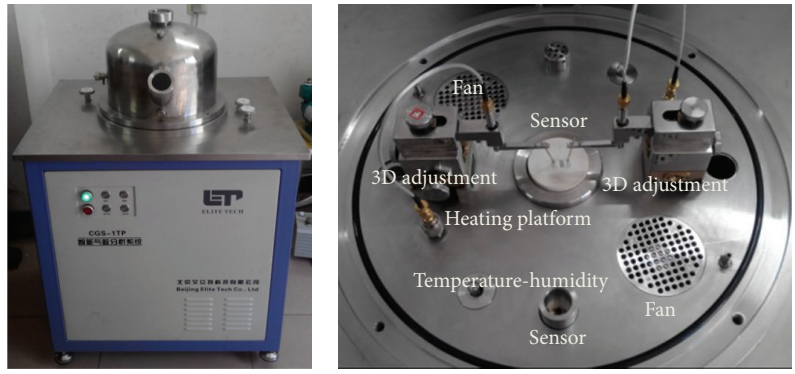

Figure 2: (a) The CGS-1TP gas sensing analysis system and (b) a photography of the operating platform.

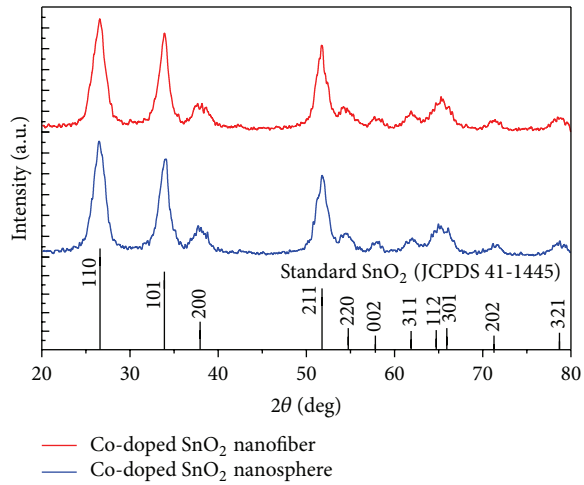

Figure 3: XRD diffraction patterns of the prepared ZnO nanostructures.

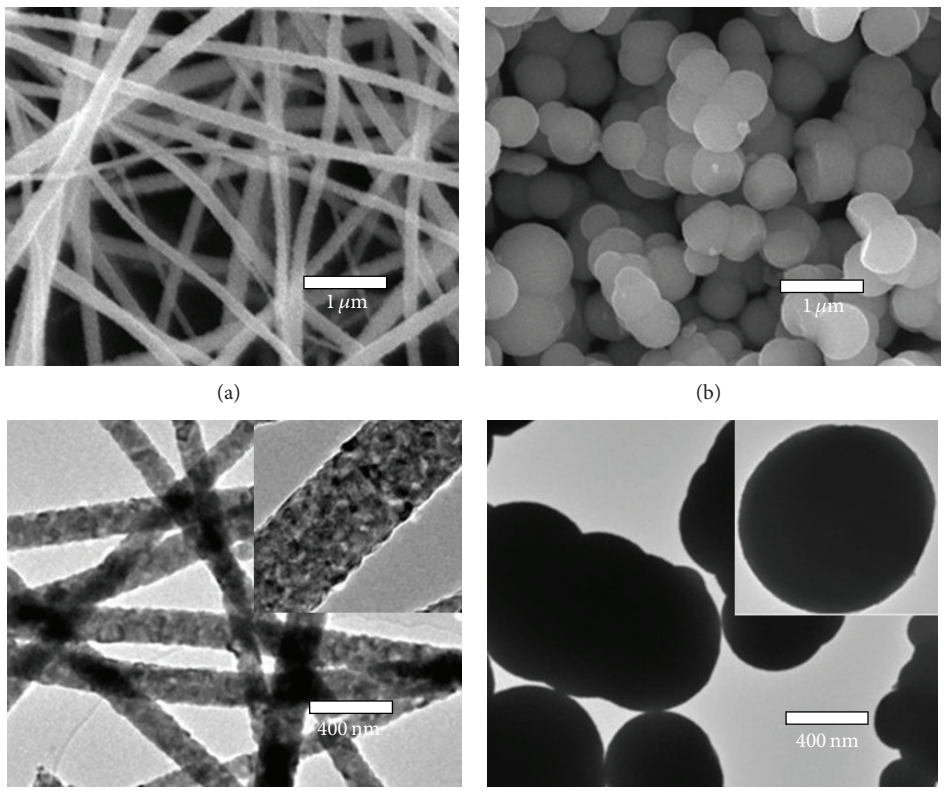

FIGURE 4: SEM images of (a) nanofibers, (b) nanospheres and TEM images of (c) nanofibers, (d) nanospheres. The inserts show the TEM images of individual fiber and sphere.

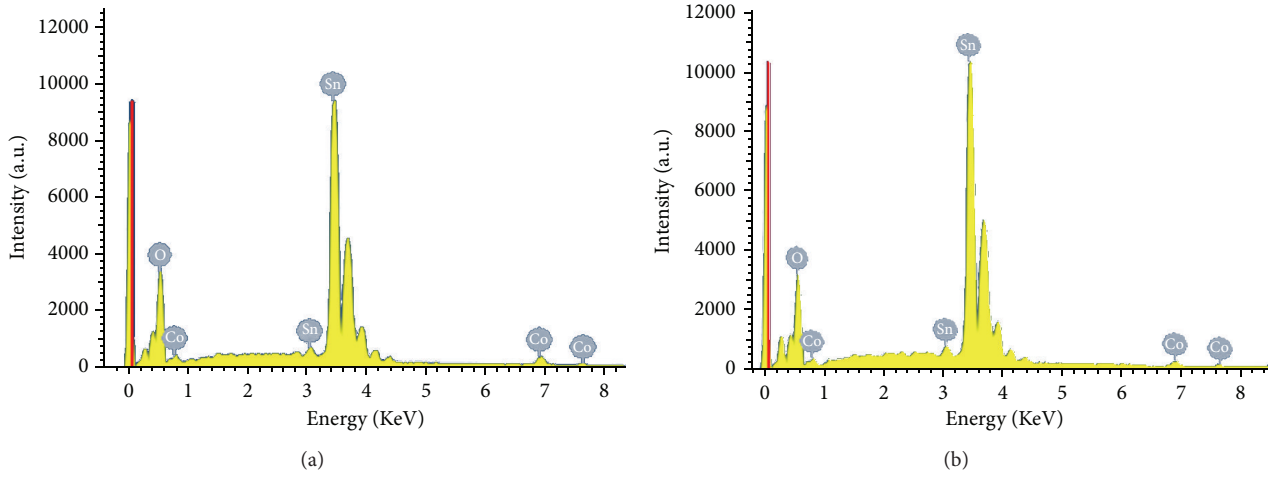

FIGURE 5: EDS spectra of 3 at% Co-doped SnO_2 (a) nanofibers and (b) nanospheres.

nanostructures that are exceptionally long in length, uniform in diameter, and large in surface area.

On the other hand, doping oxide sensors with various elements, for example, noble metals [33], rare-earth metals [34, 35], transition metals [36–38], and metal oxides [39–41], has been proved to be another effective method to improve sensing properties. Transition metal Co is a widely used dopant which acts as an activating catalyst to accelerate the chemical reaction process and consequently improve the performances [42–44]. Up to now, there are many reports on synthesis of 1D SnO_2 nanofibers and their gas sensing properties. However, most of these gas sensors focus on HCHO [45], C_2H_5OH [46, 47], C_6H_5OH [13], CO [48], NO [49], H_2 [44], H_2S [50], and NH_3 [11], and rare studies concern CH_4, a very important fault characteristic gas for transformer fault diagnosis and condition assessment. Meanwhile, a systematic

comparison of gas sensing performances between 1D SnO_2 nanofibers and traditional nanospheres may be one missing possibility along this direction.

In this paper, we reported a simple and facile approach to fabricate high-quality Co-doped SnO_2 nanofibers by electrospinning. Gas sensors were fabricated with the synthesized SnO_2 nanostructures and their sensing properties toward CH_4 are systematically investigated. The as-prepared Co-doped SnO_2 nanofibers exhibit excellent sensing characteristics, such as high sensitivity, rapid response-recovery time, and good stability than that of traditional nanospheres.

2. Experimental

Ethanol (>95%), N, N-dimethyl formamide (>95%, DMF), $CoCl_2{\cdot}2H_2O$, and $SnCl_2{\cdot}2H_2O$ were used and purchased from Chongqing Chuandong Chemical Reagent Co., Ltd (China). Poly(vinyl pyrrolidone) (PVP, Mw = 1,300,000) was obtained from Aldrich. All chemicals were analytical grade and used as received without any further purification.

In a typical procedure of Co-doped SnO_2 nanofibers [11, 13, 15, 26, 29], 0.4 g of $SnCl_2{\cdot}2H_2O$ was dissolved in 4.42 g of DMF and 4.42 g of ethanol under vigorous stirring at 90°C for 30 min. Subsequently, 1.0 g PVP and appropriate quantity of $CoCl_2{\cdot}2H_2O$ (3 at%) were added into the above solution under vigorous stirring for 2 h until the salt was completely dissolved. Then the well-mixed precursor solution was loaded into a glass syringe with a needle of 1 mm in diameter at the tip and connected to a high-voltage DC power supply (ES 30-0.1P, Gamma High Voltage Research Inc.), which was capable of generating DC voltages of up to 30 kV. In our experiment, an optimal voltage of 10 kV was provided between the tip of the spinning nozzle and the collector at a distance of 20 cm. Finally, the fibers were peeled off from the collector with tweezers and placed in a crucible. The conversion of tin dichloride to SnO_2 and the removal of organic constituents PVP in the as-spun nanofibers were achieved by calcining at 600°C for 5 h in air.

Traditional Co-doped SnO_2 nanospheres (3 at%) were synthesized via hydrothermal method and the synthesis process is similar to our previous works [6, 12, 40]. Typically, 20 mL of absolute ethanol and distilled water (V/V, 1/1), 3.0 mmol $SnCl_2{\cdot}2H_2O$, 0.09 mmol $CoCl_2{\cdot}2H_2O$, and 20 mmol ammonia hydroxide were mixed together in a 100 mL capacity beaker and magnetically stirred at room temperature for 60 min. Then the fully mixed precursor was transferred into a 50 mL Teflon-lined stainless steel autoclave, sealed, and heated at 180°C for 16 h in an electric furnace for hydrothermal reaction. Finally, the product was harvested by centrifugation, washed with distilled water and absolute ethanol several times, and dried at 100°C in air for 24 h.

The crystalline structures of the prepared SnO_2 nanofibers and nanospheres were investigated by X-ray powder diffraction (XRD, Rigaku D/Max-1200X) with Cu Kα radiation (40 kV, 200 mA and λ = 1.5418 Å). The microstructures and morphologies were characterized by means of field emission scanning electron microscope (FESEM, Hillsboro equipped with energy dispersive X-ray (EDS) spectroscopy) and transmission electron micrographs (TEM, Hitachi S-570). Analysis of the X-ray photoelectron spectra (XPS) was performed on an ESCLAB MKII using Al as the exciting source.

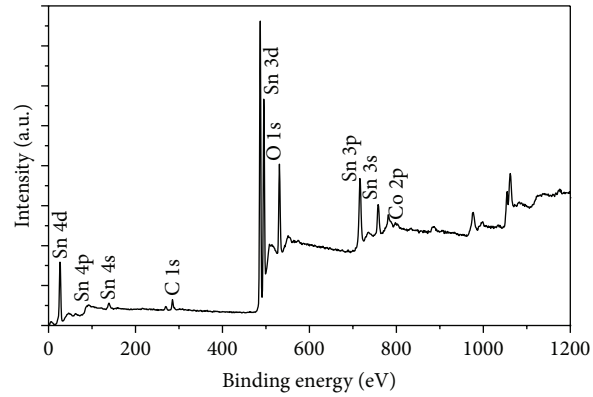

Figure 6: XPS survey spectra of 3 at% Co-doped SnO_2 nanofibers.

Gas sensors were fabricated by screen-printing technique with planar ceramic substrates, purchased from Beijing Elite Tech Co., Ltd, China. Figure 1 shows the schematic diagram of the planar sensor. It can be clearly seen in Figure 1 that the sensor consists of three kinds of significant components: ceramic substrate, Ag-Pd interdigital electrodes, and sensing materials. The length, width, and height of the planar ceramic substrate are suggested to be about 13.4, 7, and 1 mm, respectively. The as-prepared nanostructures were mixed with deionized water and absolute ethanol in a weight ratio of 100 : 20 : 10 to form a paste. Then the paste was subsequently screen-printed onto the planar ceramic substrate to form a sensing film with a thickness of about 50 μm. Finally, the fabricated sensor was dried in air at 80°C to volatilize the organic solvent and further aged in an aging test chamber for 36 h.

Gas sensing properties were investigated by a Chemical Gas Sensor-1 Temperature Pressure (CGS-1TP) intelligent gas sensing analysis system (Beijing Elite Tech Co., Ltd.) [41]. It could offer an external temperature control ranging from room temperature to 500°C with adjustment precision of 1°C. As seen in Figure 2(b) two adjustable probes were pressed on the sensor electrodes to collect electrical signals. When the sensor resistance was stable, certain amount of target gas was injected into the test chamber (18 L in volume) by a microinjector through a rubber plug. After its resistance value reached a new constant value, the test chamber was opened to recover. The sensor resistance and sensitivity were collected and analyzed by the system. And the environmental temperature, relative humidity, and working temperature were automatically recorded by the analysis system.

The sensitivity (S) was defined as $S = R_a/R_g$ [11, 13], where R_a was the sensor resistance in air and R_g in a mixture of target gas and air. The time taken by the sensor to achieve 90% of the total resistance change was designated as the response time in the case of gas adsorption or the recovery time in the case of gas desorption.

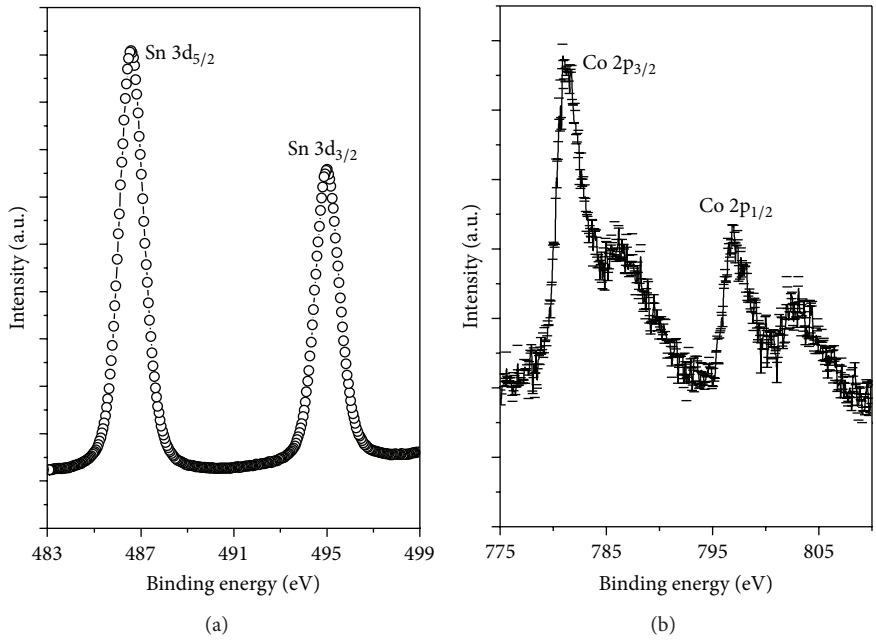

FIGURE 7: The Sn 3d (a) and Co 2p (b) binding energy spectra of 3 at% Co-doped SnO_2 nanofibers.

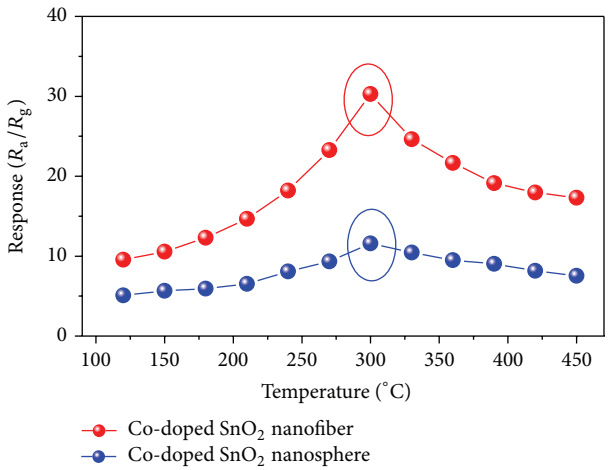

FIGURE 8: Responses of the SnO_2-based sensors to 50 ppm of CH_4 at different operating temperatures.

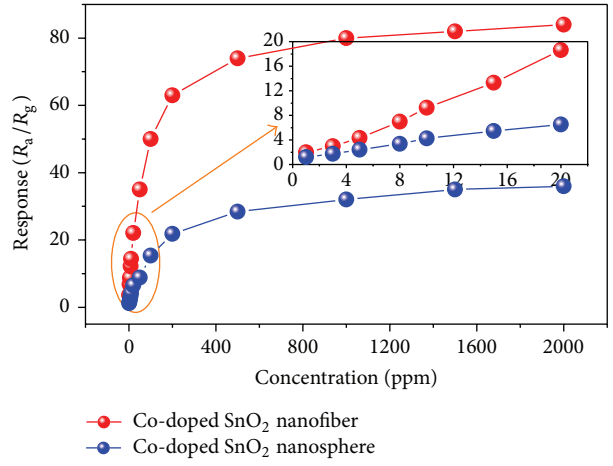

FIGURE 9: Responses of the SnO_2-based sensors to different concentrations of CH_4 at 300°C; the inserts show the relationship in the range of 1–20 ppm.

3. Results and Discussion

Figure 3 shows the XRD patterns of the as-prepared Co-doped SnO_2 nanofibers and nanospheres after calcinations. It can be clearly seen in Figure 3 that the synthesized samples are polycrystalline in nature. The prominent peaks of (110), (101), and (211) and other smaller peaks coincide with the corresponding peaks of rutile SnO_2 given in the standard data file (JCPDS File no. 41-1445). Due to the high dispersion and the low amount of Co ions (3 at%) doped in the synthesized samples, there is no indication of the presence of Co or other metal oxide diffraction peaks, implying a high purity of our products.

The overall surface morphologies of the products were performed firstly by SEM as shown in Figures 4(a) and 4(b). As shown in Figure 4(a) the disordered and bended nanofibers are randomly distributed to form a fibrous nonwoven. The average diameter of the as-spun nanofibers ranges from 200 to 120 nm, and the length of the fibers ranges from hundreds of nanometers to several ten micrometers. Figure 4(b) displays the typical SEM image of Co-doped SnO_2 nanospheres, where one can clearly note that the beautiful nanospheres are uniformly distributed across the whole sample and no other morphologies are detected. These nanospheres are rather dispersed and highly uniform in size and shape with an average diameter of 500 nm. Further

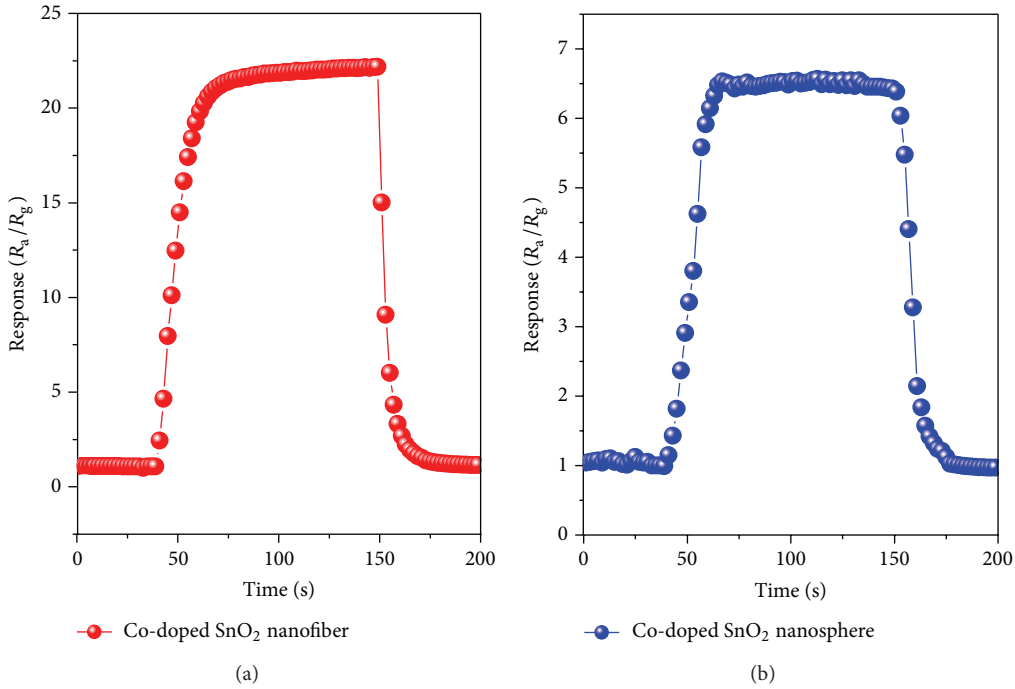

Figure 10: Response transients of Co-doped SnO_2 nanofibers (a) and nanospheres to 20 ppm of CH_4 at 300°C.

morphology characterization was examined by TEM and shown in Figures 4(c) and 4(d). The insets present the corresponding TEM images of individual fiber and sphere.

To check whether dopants have been successfully doped into the synthesized nanostructures, energy dispersive X-ray spectroscopy (EDS) measurement was conducted. Figures 5(a) and 5(b) show the EDS spectra of the as-prepared 3 at% Co-doped SnO_2 nanofibers and nanospheres, which confirm the availability of Co dopant on the SnO_2 matrix.

To further verify the existence of Co element and its valences in the synthesized samples, XPS data of the as-spun SnO_2 nanofibers is collected and presented in Figures 6 and 7. Figure 6 shows the wide spectrum, confirming the existence of Sn, O, and Co. The binding energies in Figure 7(a) at 486.5 and 493.8 eV correspond to Sn^{4+} of SnO_2. From the narrow spectrum of Co element as shown in Figure 7(b), the peak at 780.7 and 796.8 eV is identified as Co $2p_{3/2}$ and $2p_{1/2}$, respectively, which possibly can be attributed to Co^{2+} ions [8]. Meanwhile the positions of the Co $2p_{3/2}$ and Co $2p_{1/2}$ peaks ruled out the presence of metallic Co and Co_2O_3 in the Co-doped SnO_2 nanofibers [9]. Moreover, the composition of the Co dopant in our products is calculated to be about 2.88 at%, which matches well its nominal concentration. Thus, based on the EDS and XPS results, the Co^{2+} ions are believed to be successfully incorporated into the SnO_2 nanocrystals.

The responses of the nanofiber and nanosphere sensors to 50 ppm of CH_4 gas as a function of operating temperature are measured and shown in Figure 8. For each sensor, the response is measured to increase rapidly with increasing operating temperature and arrive to the maximum and then decreases with a further rise of the operating temperature. The optimum operating temperatures of the nanofibers and nanospheres are both suggested to be about 300°C with response values of 30.28 and 11.59, respectively.

The concentration dependence of Co-doped SnO_2 nanofibers and nanospheres was investigated in the range of 1–2000 ppm of CH_4 and the plots of the gas response against gas concentration are shown in Figure 9. As displayed in Figure 9, the gas response increases linearly with increasing the CH_4 concentration below 100 ppm but increases more slowly from 100 to 500 ppm, which indicates that the sensor becomes more or less saturated. Finally, the sensor reaches saturation after exposure to more than 2000 ppm. Although a similar trend was also observed for pure Co-doped SnO_2 nanospheres, the responses are much weaker. The inset in Figure 9 shows the response characteristics of the sensors to 1–20 ppm of CH_4, which indicates that the nanofibers sensor is much more favorable to detect CH_4 with a low concentration.

It is well known that response and recovery characteristics are important for evaluating the performances of semiconductor oxide sensors. Figure 10 shows the response transients of the two sensors exposed to 20 ppm of CH_4 gas at 300°C. According to the response-recovery time definition in Section 2, the response time and recovery time of nanofibers sensor were calculated to be 15 s and 12 s, and they were 22 s and 18 s for nanospheres.

To investigate the stability and repeatability of the Co-doped SnO_2 nanofibers sensor, it was sequentially exposed to different levels of CH_4 gas as shown in Figure 11 (3, 5, 8, 10, 20, and 50 ppm) and equal concentration as shown in Figure 12 (20, 20, 20, 20, and 20 ppm). As shown in Figures 11 and 12, the sensor response increases rapidly when exposed to certain concentration of CH_4 and decreases dramatically

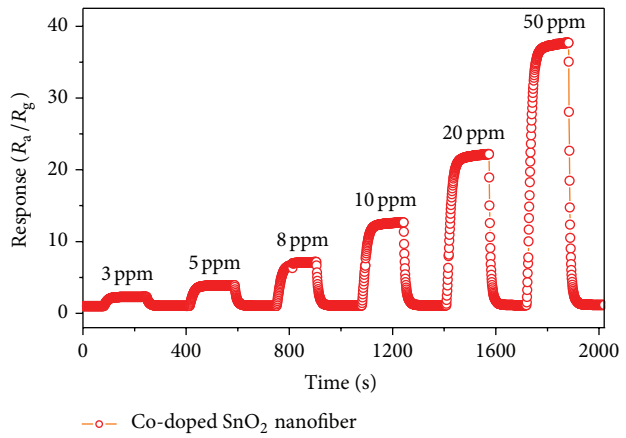

FIGURE 11: Dynamic CH_4 sensing transients of the Co-doped SnO_2 nanofiber sensor at 300°C.

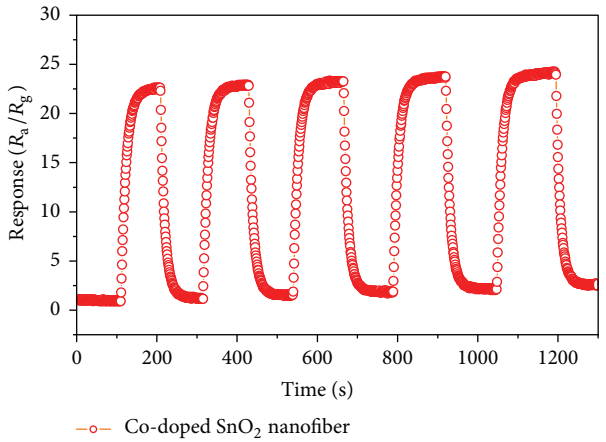

FIGURE 12: Reproducibility of the Co-doped SnO_2 nanofiber sensor on successive exposure (5 cycles) to 20 ppm of CH_4 at 300°C.

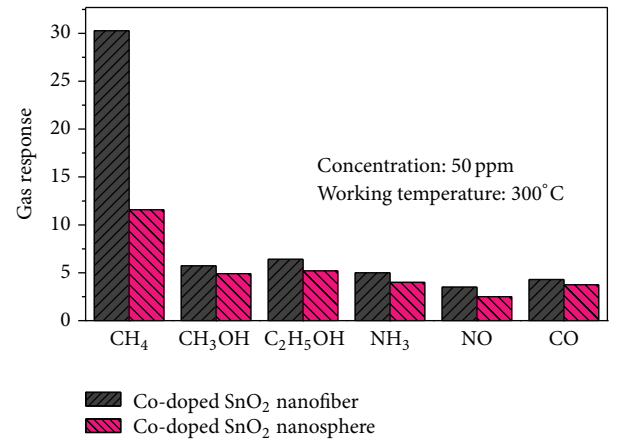

FIGURE 13: Selectivity of the Co-doped SnO_2 nanofiber sensor on successive exposure to 20 ppm of various gases at 300°C.

when exposed to air for recovering. Meanwhile, the gas response of the sensor always returns to its initial value during the continuous test period, implying a very satisfying reproducibility of the prepared sensor.

Figure 13 depicts the histogram of the gas response of the Co-doped SnO_2 nanofiber sensor to 50 ppm of various gases, including CH_4, CH_3OH, C_2H_5OH, NH_3, NO, and CO at 300°C. One can clearly see in Figure 13 that this sensor shows obvious CH_4 sensing response than other potential interface gases, which can be mainly attributed to the effect of sensor operating temperature on the activity of gas molecules.

A possible sensing mechanism is depicted as follows to understand the gas sensing reaction process of SnO_2-based sensor against CH_4 gas and explain the enhanced CH_4 sensing properties of the as-spun nanofibers. It is well known to all that SnO_2 belongs to typical n-type semiconductor sensing materials and its sensing properties are dominantly controlled by the change of SnO_2 surface resistance, especially the adsorption and desorption of oxygen on the surface of sensing materials [5]. Owing to the nonstoichiometry of the as-synthesized SnO_2 nanostructures, many oxygen vacancies are formed in SnO_2 crystal [6]. When the sensor is aged in ambient air, free oxygen could be absorbed on its surface and act as a trap capturing electrons from the conduction band of SnO_2 to generate chemisorbed oxygen species, namely, O_2^-, O^{2-}, and O^-. These chemisorbed oxygen species would cause an energy band bending of SnO_2 and depletion layers are formed around the surface area, increasing the energy barrier of SnO_2 and decreasing its carrier concentration and electron mobility [11]. Thus, a less conductive SnO_2-based sensor is measured. When the sensor is exposed to ambient CH_4, chemical reactions take place between the CH_4 molecules and the chemisorbed O_2^-, O^{2-}, and O^-, which releases the trapped electrons back to the conduction band, increasing the carrier concentration and electron mobility; thus a decreased resistance is found in our measurements [12].

Many former papers have reported and demonstrated that Co is an effective dopant to improve the gas sensing properties of metal oxide semiconductor materials, which is mainly due to the excellent electronic and chemical sensitization [42–44]. The improved CH_4 sensing properties of Co-doped SnO_2 nanofibers measured above are mainly based on the unique fiber structure [13]. Compared with traditional nanospheres, the as-spun 1D SnO_2 nanofibers possess larger surface to volume ratio, providing much more reaction sites for the target gas adsorption. Moreover, there are many nanofiber-nanofiber junctions in the netlike SnO_2 nanofibers [43]. Such junctions could form a depleted layer around the intersection, which promotes the oxygen species adsorption onto the interfacial region significantly. Then electron capture and release could undergo in a relatively easier way, accelerating the electron flow; as a result, more efficient charge transfer takes places and enhanced CH_4 sensing properties are observed.

4. Conclusions

In that summary, 3 at% Co-doped SnO_2 nanofibers have been synthesized via a simple electrospinning method and characterized by XRD, SEM, TEM, EDS, and XPS. The as-spun 3 at% Co-doped SnO_2 nanofibers exhibit high sensitivity,

supersaturated detection concentration, and rapid response and recovery against CH_4 than that of 3 at% Co-doped SnO_2 nanospheres, prepared by traditional hydrothermal synthesis route. In addition, the nanofiber sensor demonstrates excellent selectivity, prominent stability, and good reproducibility to CH_4. All results suggest that the as-spun 3 at% Co-doped SnO_2 nanofibers sensors are potential candidates for CH_4 detection. Furthermore, this method may be extendable to develop high performance semiconductor sensors monitoring other fault characteristic gases dissolved in transformer oil.

Acknowledgments

This work has been supported in part by the National Natural Science Foundation of China (no. 51277185 and 51202302), National Special Fund for Major Research Instrumentation Development (no. 2012YQ16000705), and the Funds for Innovative Research Groups of China (no. 51021005).

References

[1] J. Yu, D. Zhao, X. L. Xu, X. Wang, and N. Zhang, "Study on RuO_2/SnO_2: novel and active catalysts for CO and CH_4 oxidation," *ChemCatChem*, vol. 4, no. 8, pp. 1122–1132, 2012.

[2] J. F. Qian, P. Liu, Y. Xiao et al., "TiO_2-coated multilayered SnO_2 hollow microspheres for dye-sensitized solar cells," *Advanced Materials*, vol. 21, no. 36, pp. 3663–3667, 2009.

[3] L.-B. Luo, F.-X. Liang, and J.-S. Jie, "Sn-catalyzed synthesis of SnO_2 nanowires and their optoelectronic characteristics," *Nanotechnology*, vol. 22, no. 48, Article ID 485701, 2011.

[4] J. S. Chen, L. A. Archer, and X. W. D. Lou, "SnO_2 hollow structures and TiO_2 nanosheets for lithium-ion batteries," *Journal of Materials Chemistry*, vol. 21, no. 27, pp. 9912–9924, 2011.

[5] W. Zeng, T. M. Liu, D. J. Liu, and E. J. Han, "Hydrogen sensing and mechanism of M-doped SnO_2 ($M=Cr^{3+}$, Cu^{2+} and Pd^{2+}) nanocomposite," *Sensors and Actuators B*, vol. 160, no. 1, pp. 455–462, 2011.

[6] W. G. Chen, Q. Zhou, T. Y. Gao, X. P. Su, and F. Wan, "Pd-doped SnO_2-based sensor detecting characteristic fault hydrocarbon gases in transformer oil," *Journal of Nanomaterials*, vol. 2013, Article ID 127345, 9 pages, 2013.

[7] H. Huang, C. K. Lim, M. S. Tse, J. Guo, and O. K. Tan, "SnO_2 nanorod arrays: low temperature growth, surface modification and field emission properties," *Nanoscale*, vol. 4, no. 5, pp. 1491–1496, 2012.

[8] K. Srinivas, M. Vithal, B. Sreedhar, M. M. Raja, and P. V. Reddy, "Structural, optical, and magnetic properties of nanocrystalline Co doped SnO_2 based diluted magnetic semiconductors," *The Journal of Physical Chemistry C*, vol. 113, no. 9, pp. 3543–3552, 2009.

[9] X. F. Liu, J. Iqbal, S. L. Yang, B. He, and R. H. Yu, "Nitrogen doping-mediated room-temperature ferromagnetism in insulating Co-doped SnO_2 films," *Applied Surface Science*, vol. 256, no. 14, pp. 4488–4492, 2010.

[10] W. G. Chen, Q. Zhou, F. Wan, and T. Y. Gao, "Gas sensing properties and mechanism of nano-SnO_2-based sensor for hydrogen and carbon monoxide," *Journal of Nanomaterials*, vol. 2012, Article ID 612420, 9 pages, 2012.

[11] H. G. Zhang, Z. Y. Li, L. Liu et al., "Enhancement of hydrogen monitoring properties based on Pd-SnO_2 composite nanofibers," *Sensors and Actuators B*, vol. 147, no. 1, pp. 111–115, 2010.

[12] Q. Qi, T. Zhang, L. Liu, X. J. Zheng, and G. Y. Lu, "Improved NH_3, C_2H_5OH, and CH_3COCH_3 sensing properties of SnO_2 nanofibers by adding block copolymer P123," *Sensors and Actuators B*, vol. 141, no. 1, pp. 174–178, 2009.

[13] K. J. Choi and H. W. Jang, "One-dimensional oxide nanostructures as gas-sensing materials: review and issues," *Sensors*, vol. 10, no. 4, pp. 4083–4099, 2010.

[14] Q. Qi, T. Zhang, L. Liu, and X. J. Zheng, "Synthesis and toluene sensing properties of SnO_2 nanofibers," *Sensors and Actuators B*, vol. 137, no. 2, pp. 471–475, 2009.

[15] W. G. Chen, Q. Zhou, and S. D. Peng, "Hydrothermal synthesis of Pt-, Fe-, and Zn-doped SnO_2 nanospheres and carbon monoxide sensing properties," *Advances in Materials Science and Engineering*, vol. 2013, Article ID 578460, 8 pages, 2013.

[16] Z. J. Wang, Z. Y. Li, T. T. Jiang, X. R. Xu, and W. Wang, "Ultrasensitive hydrogen sensor based on Pd^0-loaded SnO_2 electrospun nanofibers at room temperature," *ACS Applied Materials & Interfaces*, vol. 5, no. 6, pp. 2013–2021, 2013.

[17] L. L. Wang, H. M. Dou, Z. Lou, and T. Zhang, "Encapsuled nanoreactors (Au@ SnO_2): a new sensing material for chemical sensors," *Nanoscale*, vol. 5, no. 7, pp. 2686–2691, 2011.

[18] J. Fang, H. T. Niu, T. Lin, and X. G. Wang, "Applications of electrospun nanofibers," *Chinese Science Bulletin*, vol. 53, no. 15, pp. 2265–2286, 2008.

[19] S. Barth, F. Hernandez-Ramirez, J. D. Holmes, and A. Romano-Rodriguez, "Synthesis and applications of one-dimensional semiconductors," *Progress in Materials Science*, vol. 55, no. 6, pp. 563–627, 2010.

[20] Y. N. Xia, P. D. Yang, Y. G. Sun et al., "One-dimensional nanostructures: synthesis, characterization, and applications," *Advanced Materials*, vol. 15, no. 5, pp. 353–389, 2003.

[21] J. G. Lu, P. C. Chang, and Z. Y. Fan, "Quasi-one-dimensional metal oxide materials-synthesis, properties and applications," *Materials Science and Engineering R*, vol. 52, no. 1–3, pp. 49–91, 2006.

[22] Y. J. Chen, X. Y. Xue, Y. G. Wang, and T. H. Wang, "Synthesis and ethanol sensing characteristics of single crystalline SnO_2 nanorods," *Applied Physics Letters*, vol. 87, no. 23, Article ID 233503, pp. 1–3, 2005.

[23] Z. W. Pan, Z. R. Dai, and Z. L. Wang, "Nanobelts of semiconducting oxides," *Science*, vol. 291, no. 5510, pp. 1947–1949, 2001.

[24] B. Wang, L. F. Zhu, Y. H. Yang, N. S. Xu, and G. W. Yang, "Fabrication of a SnO_2 nanowire gas sensor and sensor performance for hydrogen," *The Journal of Physical Chemistry C*, vol. 112, no. 17, pp. 6643–6647, 2008.

[25] Y. B. Shen, T. Yamazaki, Z. F. Liu et al., "Microstructure and H_2 gas sensing properties of undoped and Pd-doped SnO_2 nanowires," *Sensors and Actuators B*, vol. 135, no. 2, pp. 524–529, 2009.

[26] C. Wang, Y. Zhou, M. Y. Ge, X. B. Xu, Z. Zhang, and J. Z. Jiang, "Large-scale synthesis of SnO_2 nanosheets with high lithium storage capacity," *Journal of the American Chemical Society*, vol. 132, no. 1, pp. 46–47, 2010.

[27] Y. Zhang, X. He, J. Li, Z. Miao, and F. Huang, "Fabrication and ethanol-sensing properties of micro gas sensor based on electrospun SnO_2 nanofibers," *Sensors and Actuators B*, vol. 132, no. 1, pp. 67–73, 2008.

[28] X. Song, Z. Wang, Y. Liu, C. Wang, and L. Li, "A highly sensitive ethanol sensor based on mesoporous ZnO-SnO_2 nanofibers," *Nanotechnology*, vol. 20, no. 7, Article ID 075501, 2009.

[29] T. Lin, D. Lukas, and G. S. Bhat, "Nanofiber manufacture, properties, and applications," *Journal of Nanomaterials*, vol. 2013, 1 page, Article ID 368191, 2013.

[30] J. Doshi and D. H. Reneker, "Electrospinning process and applications of electrospun fibers," *Journal of Electrostatics*, vol. 35, no. 2-3, pp. 151–160, 1995.

[31] Z. R. Dai, Z. W. Pan, and Z. L. Wang, "Novel nanostructures of functional oxides synthesized by thermal evaporation," *Advanced Functional Materials*, vol. 13, no. 1, pp. 9–24, 2003.

[32] L. Tan, L. Wang, and Y. Wang, "Hydrothermal synthesis of SnO_2 nanostructures with different morphologies and their optical properties," *Journal of Nanomaterials*, vol. 2011, Article ID 529874, 10 pages, 2011.

[33] Y. Liu, E. Koep, and M. Liu, "A highly sensitive and fast-responding SnO_2 sensor fabricated by combustion chemical vapor deposition," *Chemistry of Materials*, vol. 17, no. 15, pp. 3997–4000, 2005.

[34] L. L. Wang, Z. Lou, R. Wang, T. Fei, and T. Zhang, "Ring-like PdO-NiO with lamellar structure for gas sensor application," *Journal of Materials Chemistry*, vol. 22, no. 25, pp. 12453–12456, 2012.

[35] H. Bastami, E. Taheri-Nassaj, P. F. Smet, K. Korthout, and D. Poelman, "(Co, Nb, Sm)-doped tin dioxide varistor ceramics sintered using nanopowders prepared by coprecipitation method," *Journal of the American Ceramic Society*, vol. 94, no. 10, pp. 3249–3255, 2011.

[36] Q. Qi, T. Zhang, X. Zheng et al., "Electrical response of Sm_2O_3-doped SnO_2 to C_2H_2 and effect of humidity interference," *Sensors and Actuators B*, vol. 134, no. 1, pp. 36–42, 2008.

[37] W. Zeng, T. Liu, Z. Wang, S. Tsukimoto, M. Saito, and Y. Ikuhara, "Selective detection of formaldehyde gas using a Cd-doped TiO_2-SnO_2 sensor," *Sensors*, vol. 9, no. 11, pp. 9029–9038, 2009.

[38] X. Liu, J. Zhang, X. Guo, S. Wu, and S. Wang, "Enhanced sensor response of Ni-doped SnO_2 hollow spheres," *Sensors and Actuators B*, vol. 152, no. 2, pp. 162–167, 2011.

[39] K. M. Kim, H. M. Jeong, H. R. Kim, K. Choi, H. J. Kim, and J. H. Lee, "Selective detection of NO_2 using Cr-doped CuO nanorods," *Sensors*, vol. 12, no. 6, pp. 8013–8025, 2012.

[40] Z. Lou, J. N. Deng, L. L. Wang, R. Wang, T. Fei, and T. Zhang, "A class of hierarchical nanostructures: ZnO surface-functionalized TiO_2 with enhanced sensing properties," *RSC Advances*, vol. 3, no. 9, pp. 3131–3136, 2013.

[41] W. Zeng, T. Liu, and Z. Wang, "Enhanced gas sensing properties by SnO_2 nanosphere functionalized TiO_2 nanobelts," *Journal of Materials Chemistry*, vol. 22, no. 8, pp. 3544–3548, 2012.

[42] X.-J. Zhang and G.-J. Qiao, "High performance ethanol sensing films fabricated from ZnO and In_2O_3 nanofibers with a double-layer structure," *Applied Surface Science*, vol. 258, no. 17, pp. 6643–6647, 2012.

[43] Z. Li and Y. Dzenis, "Highly efficient rapid ethanol sensing based on Co-doped In_2O_3 nanowires," *Talanta*, vol. 85, no. 1, pp. 82–85, 2011.

[44] L. Liu, S. Li, J. Zhuang et al., "Improved selective acetone sensing properties of Co-doped ZnO nanofibers by electrospinning," *Sensors and Actuators B*, vol. 155, no. 2, pp. 782–788, 2011.

[45] L. Liu, C. Guo, S. Li, L. Wang, Q. Dong, and W. Li, "Improved H_2 sensing properties of Co-doped SnO_2 nanofibers," *Sensors and Actuators B*, vol. 150, no. 2, pp. 806–810, 2010.

[46] H. Du, J. Wang, M. Su, P. Yao, Y. Zheng, and N. Yu, "Formaldehyde gas sensor based on SnO_2/In2O3 hetero-nanofibers by a modified double jets electrospinning process," *Sensors and Actuators B*, vol. 166, no. 2, pp. 746–752, 2012.

[47] L. Liu, S. C. Li, L. Y. Wang, C. C. Guo, and Q. Y. Dong, "Enhancement ethanol sensing properties of NiO-SnO_2 nanofibers," *Journal of the American Ceramic Society*, vol. 94, no. 3, pp. 771–775.

[48] X. Song and L. Liu, "Characterization of electrospun ZnO-SnO_2 nanofibers for ethanol sensor," *Sensors and Actuators A*, vol. 154, no. 1, pp. 175–179, 2009.

[49] X. J. Yue, T. S. Hong, W. Xiang, K. Cai, and X. Xu, "High performance micro CO sensors based on ZnO-SnO_2 composite nanofibers with anti-humidity characteristics," *Chinese Physics Letters*, vol. 29, no. 12, Article ID 120702, pp. 1–4, 2012.

[50] J.-A. Park, J. Moon, S.-J. Lee, S. H. Kim, H. Y. Chu, and T. Zyung, "SnO_2-ZnO hybrid nanofibers-based highly sensitive nitrogen dioxides sensor," *Sensors and Actuators B*, vol. 145, no. 1, pp. 592–595, 2010.